

ZnFe₂O₄ Doped TiO₂ Photocatalyst Synthesis and Characterization with Effect of Different Coupling Ratios on Band Gap

¹Farukh Iqbal*, ²Saad Nadeem, ³Kamran Zakaria and ¹Bawadi Abdullah

¹Department of Chemical Engineering, Universiti Teknologi PETRONAS 32610 Bandar Seri Iskandar, Perak, Malaysia.

²Department of Chemical Engineering, NED University of Engineering & Technology, Karachi, Pakistan.

³Department of Mathematics, NED University of Engineering & Technology, Karachi, Pakistan.
mfarukhiqbal@gmail.com*

(Received on 19th March 2021, accepted in revised form 22nd June 2021)

Summary: In this work the effect of different coupling ratios of ZnFe₂O₄ and TiO₂ on the band gap was investigated, to convert TiO₂ as a visible light driven photocatalyst ZnFe₂O₄. In this work, ZnFe₂O₄ was synthesized utilizing sol-gel technique and calcining under normal atmosphere at 900 °C. Thereafter, ZnFe₂O₄ was coupled with TiO₂ by mixing in 50 ml water in three different coupling w/w ratios (1:1, 1:2 and 2:1) followed by the calcination of coupled catalyst under nitrogen environment at 500 °C. XRD, XPS, FESEM-EDS imaging, TGA, UV-Vis, and FTIR were performed to characterize the catalyst. Crystal phase identification could be confirmed through XRD analysis with homogenous distribution of metal constituents through color mapping and surface charge transitions from XPS analysis for a better electron hole generation. Thermogravimetric analysis (TGA) confirmed that the pure ZnFe₂O₄ obtained at 900 °C, while FTIR verified the presence of desired functional group in ZnFe₂O₄. Moreover, Fourier Transformation Infrared Spectroscopy (FTIR) illustrated two major peaks and no extra major impurity was detected. ZnFe₂O₄ is visible light driven photocatalyst and TiO₂ can work only under UV light. So, the effect of different coupling ratios of ZnFe₂O₄ with TiO₂ was examined by UV-Vis characterization. The band gap is given by 1:1 was 2.8, 2:1 was 3.17 and 1:2 was 3.02. It was observed that the most optimum coupling ratio is 1:1 and the band-gap fall under visible region. The findings of this work could be supportive significantly for the selection of suitable coupling ratio to convert UV-driven photocatalyst into visible region active photocatalyst.

Keywords: TiO₂; ZnFe₂O₄; TGA; UV-VIS; FTIR and ratio.

Introduction

IN the current times global warming has become an important issue to scientists. The emission from automobiles and industries is the biggest source of global warming. The ultimate and promising aspect to reduce these greenhouse gases (GHGs) is to convert them in to high value chemical and fuels using a sustainable pathway *i.e.* the visible light transformation of gaseous product CO₂ into liquid fuel (methanol) [1, 2].

Visible lights make up approximately 47% of the solar radiations from Sun and only 4 to 5 % of it is comprised of UV light. Due to the constraints that the solar energy is not able to transform CO₂ into valuable fuels due to the energy barrier or endothermic nature of the reaction, an external energy source is required which can be fulfilled by using a photocatalyst in order to overcome this energy barrier [3]. A vast majority of photocatalyst materials offer high band gap values and are active under the UV region of the solar radiation. The obvious distinction which determines either the photocatalyst is visible or UV light-driven depending

upon its band gap. A photocatalyst will work visible light driven if its band gap less than 2 eV.

Metal ferrites have emerged as an excellent alternative to this problem as photocatalyst materials owing to the low values of band gap and capacity to utilize the solar radiation visible region [4-6]. The problem with using photocatalyst with low band gap value is the potential of high electron hole recombination rate. Doping of various materials have been conducted in order to decelerate the electron hole recombination process while allowing the photocatalyst material to complete the reaction cycle to synthesize liquid products [7-10]. The following characteristic should be portrayed by a photocatalyst through semiconductor-semiconductor coupling technique, the conduction band position of small band gap semiconductor should be more negative [11, 12]. As suggested by literature review, ZnFe₂O₄ is a promising candidate as a visible light driven photocatalyst material having a small band gap value [4]. TiO₂ doped ZnFe₂O₄ material has the capability to sensitize the TiO₂ counterpart thus inducing visible

*To whom all correspondence should be addressed.

light activity and charge transfer characteristic making this heterojunction material a very active visible light photocatalyst. Formation of heterojunction helps to slow down the charge recombination.

Experimental

Materials

All the chemicals which were bought, consumed deprived of any cleansing. Nitric acid (HNO_3), iron nitrate ($\text{Fe}(\text{NO}_3)_3 \cdot 9\text{H}_2\text{O}$) (99.5%), Zinc nitrate ($\text{Zn}(\text{NO}_3)_2 \cdot 6\text{H}_2\text{O}$) (99.5%), commercialized TiO_2 and Agar had been utilized to synthesize the photocatalyst material $\text{ZnFe}_2\text{O}_4/\text{TiO}_2$. The water had a resistivity of $>10^{18} \text{ M}\Omega \text{ cm}^{-1}$. All the chemicals were reagent grade.

Synthesis

The synthesis of the photocatalyst material ZnFe_2O_4 was made possible by employing the sol-gel technique as has been outlined earlier [13, 14]. Calcination of ZnFe_2O_4 was performed at 900°C . The calcined material was then doped with the TiO_2 counterpart applying the sol-gel technique. The commercialized TiO_2 with ZnFe_2O_4 were mixed in distilled water (50 ml) having the mentioned w/w (1:1, 1:2, 2:1) ratio. The resulting mixture was then kept for ultrasonication for 1 h and afterwards was placed in an oven for 12 h at a temperature of 100°C for drying. Lastly, the dried doped photocatalyst material was calcined under the presence of nitrogen gas in a tubular furnace at 500°C [15].

Characterization

The synthesized photocatalyst material ZnFe_2O_4 was characterized with the help of Ultraviolet Visible light (UV-Vis) spectroscopy, for visible light activity, Fourier Transform Infrared (FTIR) analysis with Nicolet 6700, Thermo Scientific, USA in order to identify the existence of anticipated functional group and Thermogravimetric analysis (TGA) ASTA 6000, PerkinElmer, USA for the requisite calcination conditions in order to remove all the undesirable impurities. TGA of the sample was carried out heating at a rate of $10^\circ\text{C}/\text{min}$ for appropriate calcination temperature identification. X-ray photoelectron spectroscopy (XPS) analysis employing Thermo Fisher Scientific K-Alpha system with a mono-chromatic Al $\text{K}\alpha$ source (1593 eV) of the synthesized samples was performed for the surface elemental presence of all the metals in the composite photocatalyst material. X-ray Diffraction

(XRD) patterns in the 2 theta domain from 10° till 80° with Bruker diffractometer with Cu $\text{K}\alpha$ radiation ($\lambda=0.154 \text{ nm}$) with an accelerating potential of 40 kV for the confirmation of the composite photocatalyst were also performed. The surface morphology was studied with FESEM-EDX colour mapping was performed with a Zeiss Supra 55 VP for surface morphology determination. In the end, the TiO_2 and ZnFe_2O_4 doped material having w/w ratio (1:1, 1:2, 2:1) respectively was subjected to absorbance study by employing UV-Vis spectroscopy by DR-UVS K Series spectrophotometer within a range of 200 nm to 800 nm to determine the consequence of doping ratios on band gap and absorbance.

Results and Discussion

FTIR

The FTIR analysis is provided in **Error! Reference source not found.** The spectrum reveals a similar behavior as compared to earlier reported [16]. The evident sharp decrease at 538 and 421 cm^{-1} respectively signifies the Zn^{2+} and Fe^{3+} states in the sample [16, 17]. Correspondingly, the sharp depression at 1456 cm^{-1} and 1649 cm^{-1} can be attributed to the presence of bending vibrations of water [18] portraying less concentration of OH ions of water. The comprehensive 1123 cm^{-1} band might be ascertained to the vibrational stretchings of Zn-O [17].

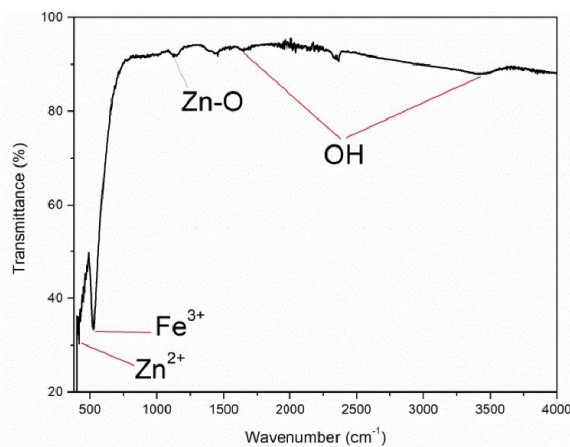


Fig. 1: FTIR Spectra of ZnFe_2O_4

XRD

The XRD analysis is provided in Fig.. And it can be seen that the composite photocatalyst material confirmed the synthesis of the photocatalyst material $\text{ZnFe}_2\text{O}_4/\text{TiO}_2$. The

synthesized structure shows complete crystal formation and no amorphous phase presence and the findings are consistent with literature [6] as well.

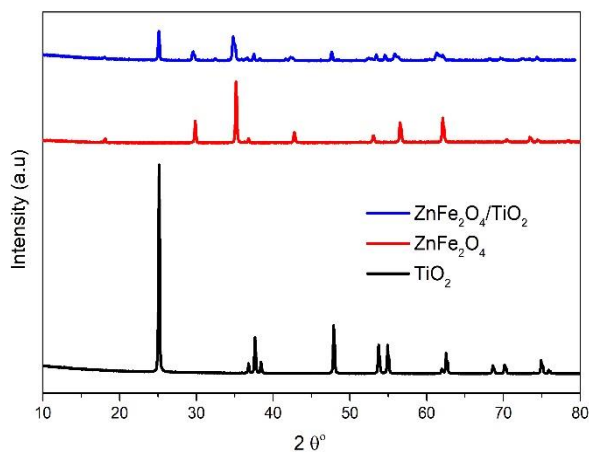


Fig. 2: XRD analysis of ZnFe_2O_4 , TiO_2 and $\text{ZnFe}_2\text{O}_4/\text{TiO}_2$.

XPS

The XPS analysis is provided in

Fig. 3, which provides the surface metal presence over the synthesized materials. It is very obvious that no Ti can be observed in the ZnFe_2O_4 sample and no Zn and Fe could be found over the surface of TiO_2 material. The coupling of ZnFe_2O_4 with TiO_2 resulted in composite material with all the elements detected by in the survey of the $\text{ZnFe}_2\text{O}_4/\text{TiO}_2$ photocatalyst material as depicted in the Fig 3 as well. The XPS confirms the formation of the target material along with the XRD analysis.

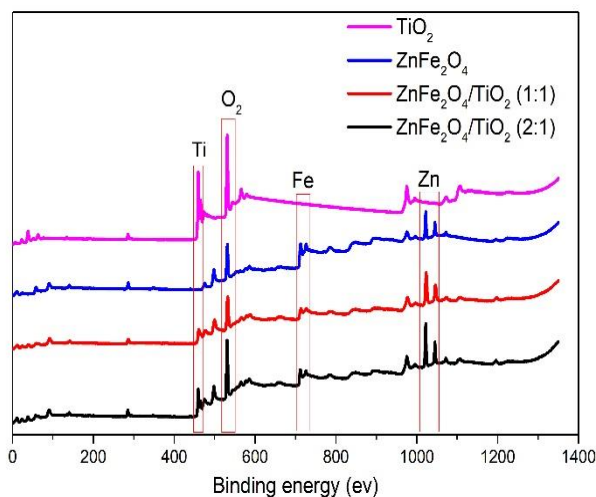


Fig. 3: XPS analysis of ZnFe_2O_4 , TiO_2 and $\text{ZnFe}_2\text{O}_4/\text{TiO}_2$.

FESEM and Colour Mapping

The FESEM image analysis for the surface morphology is given in

Fig. (a – c) respectively for ZnFe_2O_4 , TiO_2 and $\text{ZnFe}_2\text{O}_4/\text{TiO}_2$ samples.

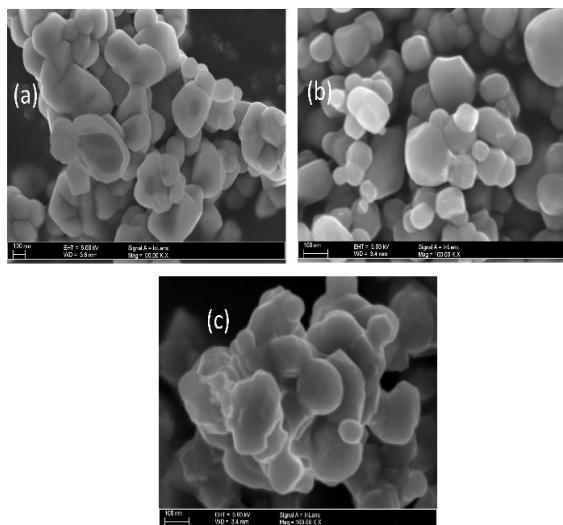


Fig. 4: FESEM images of (a) ZnFe_2O_4 , (b) TiO_2 and (c) $\text{ZnFe}_2\text{O}_4/\text{TiO}_2$.

The colour mapping is also presented in Fig. 5 for ZnFe_2O_4 , and in Fig. 6 for TiO_2 and Fig. 7 for $\text{ZnFe}_2\text{O}_4/\text{TiO}_2$ samples. The colour mapping also verifies the formation of the target molecules.

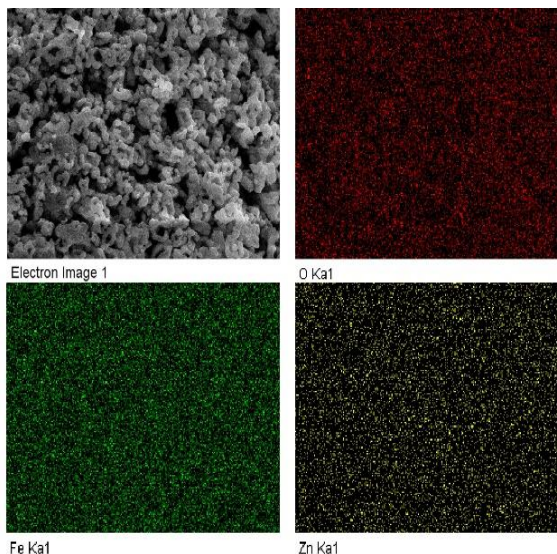
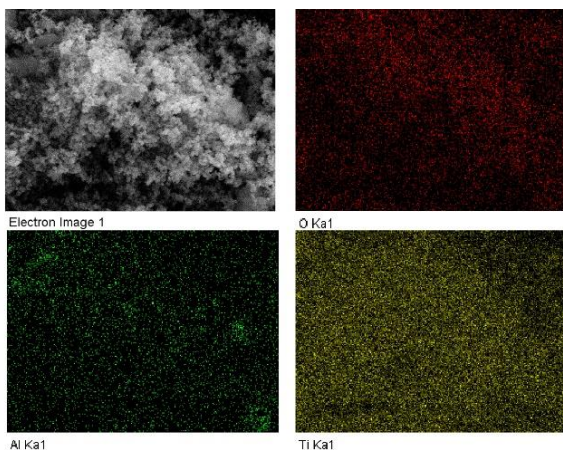
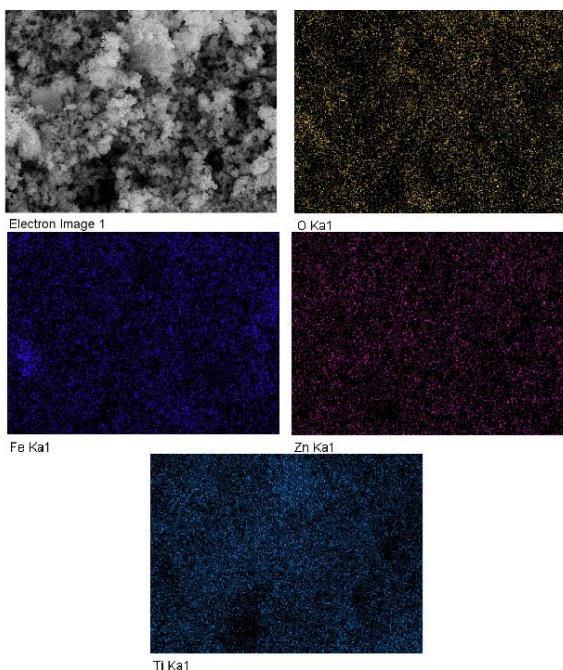


Fig. 5: Color Map images of ZnFe_2O_4 .

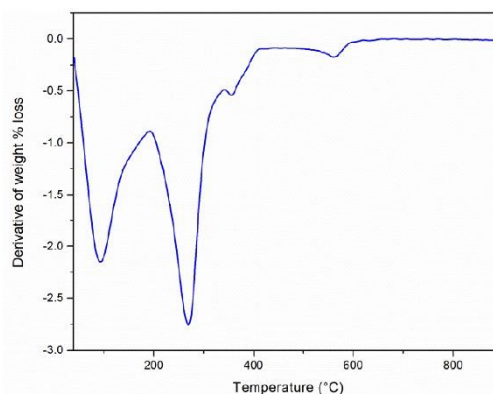
Fig. 6: Colour Map images of TiO₂.Fig. 7: Colour Map images of ZnFe₂O₄/TiO₂.

TGA

The TGA analysis is given in

Fig. which portrays the derivative profiles of ZnFe₂O₄ mass loss relating to temperature. TGA was conducted prior to calcination in order to conclude the catalyst stability with respect to increasing temperatures. The TGA of the un-calcined catalyst material sample was in agreement with our earlier work having slight disparity. In earlier work reported the 50-200 °C weight loss amounted to 10% conversely, in the current work, a 20% weight loss had been detected between the same temperature intervals. Likewise, our earlier work represented a

20% weight loss within 200-600 °C owing to the elimination of ZnO but in this study 25% weight loss was detected that can be attributed to the presence of interlayer water molecules [13]. The presence of large amount of water molecules resulted in additional time required for complete drying of the moisture content. The observed weight loss between 600 – 900 °C, was not significant. Results of this study are in agreement with the earlier reported study [4]. From the TGA analysis of samples the calcination temperature in this study was fixed at 900 °C.

Fig. 8: DTGA curve of ZnFe₂O₄.

UV-Visible Study

The UV-Visible analysis of the synthesized photocatalyst materials TiO₂ (700 °C calcination temperature) doped with ZnFe₂O₄ (900°C calcination temperature) having a (1:1, 1:2, 2:1) w/w ratio was analyzed from 200-800 nm is presented in

Fig.. The coupling of TiO₂ with ZnFe₂O₄ demonstrates a definite absorbance in the visible region *i.e.* 400-800 nm. All the synthesized samples depicted visible region absorbance nonetheless the 1:1 w/w ratio sample showed considerably greater absorbance in comparison with other ratios. 1:1 coupling ratio portrayed a promising alteration of TiO₂ band gap from UV region to the visible portion.

ZnFe₂O₄ does not simply alter the TiO₂ band gap becoming visible light active but also decreased the band gap value. From the analysis the photocatalyst with a w/w/ ratio of 1:1 was found to be most promising among the ratios effectively decreasing the band gap of the photocatalyst and presented largest absorption within visible region. The 1:1 w/w ratio doped catalyst at 760 nm displays highest band energy and can be attributed to the electron transition to the Conduction band of ZnFe₂O₄ from the ZnFe₂O₄ Valence band.

Correspondingly, the absorption at 446 nm might be ascertained to the electron transition from ZnFe_2O_4 Valance band to TiO_2 conduction band. The ZnFe_2O_4 Band-gap structure can be corresponding to the valence band (O-2p orbital) and conduction band (Fe-3d orbital) [19, 20]. The $h\nu$ value was deliberate employing Equation 1.

$$h\nu = 1240/\lambda \quad (1)$$

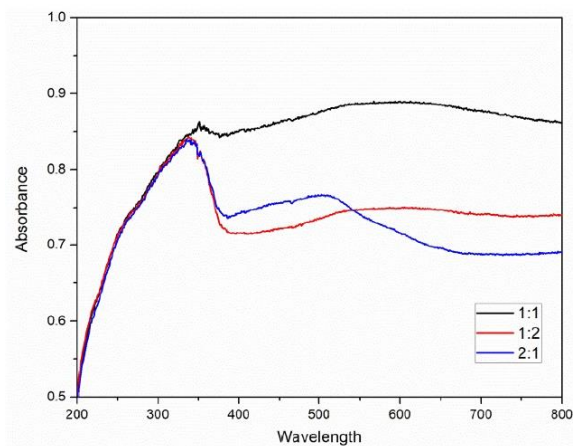


Fig. 9: Absorption spectrum of synthesized photocatalyst materials $\text{ZnFe}_2\text{O}_4/\text{TiO}_2$ (1:1), $\text{ZnFe}_2\text{O}_4/\text{TiO}_2$ (1:2) and $\text{ZnFe}_2\text{O}_4/\text{TiO}_2$ (2:1) under UV-Visible light irradiation.

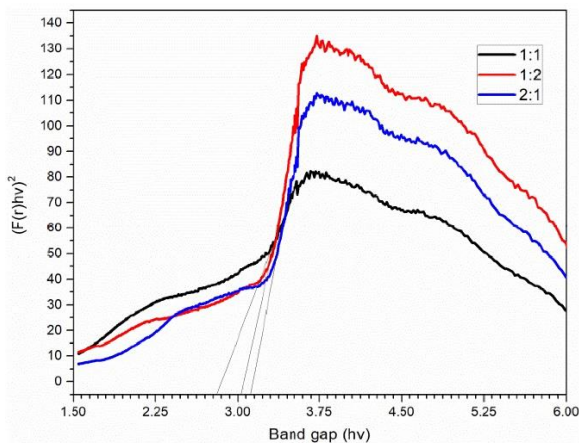


Fig. 10: Calculation of Band gap energy of synthesized catalyst.

The calculation of band-gap was made possible by plotting the tauc plot relation. The graph plotted between $h\nu$ and $(F(R).h\nu)^2$ is demonstrated in

Fig.. The extrapolation of the steep linear portion of the graph to the X-axis results in the value

of band gap of the photocatalyst which in turns identify the activity of photocatalyst in UV or Visible region. The band gap values of the synthesized samples in (1:1, 1:2, 2:1) w/w proportions were relatively found to be 2.8, 3.02 and 3.10. The TiO_2 doping with the ZnFe_2O_4 in suitable proportion relocated the TiO_2 band gap of from UV region in to the visible light region. This visible light active photocatalyst can be exploited effectively for redox reaction studies under visible light.

Conclusion

In the current study $\text{ZnFe}_2\text{O}_4/\text{TiO}_2$ hetero-junctions photocatalyst material was synthesized employing the sol-gel technique which portrayed absorbance in the visible light region of the solar spectrum. The Band gap analysis shows that the 1:1 w/w ratio is the most promising among the other ratios namely 1:2 and 2:1 for the conversion of CO_2 to hydrocarbons and valuable fuels. The XRD and XPS study also confirmed the formation of the target hetero-junction material. The FESEM and EDS image analysis further evidenced its formation. The electron hole recombination will also be altered due to heterojunction formation. Successful reduction of CO_2 into methanol could be observed from the synthesized $\text{ZnFe}_2\text{O}_4/\text{TiO}_2$ photocatalyst under the visible light region of solar spectrum.

Acknowledgements

We acknowledge all the people for their support during this study, particularly the staff and lab personnel of Chemical Engineering Department.

References

1. N. Ahmed, Y. Shibata, T. Taniguchi and Y. Izumi, Photocatalytic conversion of carbon dioxide into methanol using zinc-copper-M (III)(M= aluminum, gallium) layered double hydroxides, *J. Catal*, **279**, 1, 123 (2011).
2. S. Nadeem, A. Mumtaz, M. Mumtaz, M. A. Mutalib, M. S. Shaharun and B. Abdullah, Visible light driven CO_2 reduction to methanol by Cu-porphyrin impregnated mesoporous Ti-MCM-48, *J. Mol. Liq*, **272**, 656 (2018).
3. P. Akhter, M. A. Farkhondehfal, S. Hernández, M. Hussain, A. Fina, G. Saracco, A. U. Khan and N. Russo, Environmental issues regarding CO_2 and recent strategies for alternative fuels through photocatalytic reduction with titania-based materials, *J. Environ. Chem. Eng*, **4**, 3934 (2016).

4. M. A. Asi, C. He, M. Su, D. Xia, L. Lin, H. Deng, Y. Xiong, R. Qiu and X.-z. Li, Photocatalytic reduction of CO₂ to hydrocarbons using AgBr/TiO₂ nanocomposites under visible light, *Catal. Today*, **175**, 256, (2011).
5. E. Baeissa, Green synthesis of methanol by photocatalytic reduction of CO₂ under visible light using a graphene and tourmaline co-doped titania nanocomposites, *Ceram. Int.*, **40**, 12431 (2014).
6. F. Iqbal, A. Mumtaz, S. Shahabuddin, M. I. Abd Mutalib, M. S. Shaharun, T. D. Nguyen, M. R. Khan and B. Abdullah, Photocatalytic reduction of CO₂ to methanol over ZnFe₂O₄/TiO₂ (p-n) heterojunctions under visible light irradiation, *J. Chem. Technol. Biotechnol.*, **95**, 2208 (2020).
7. E. Casbeer, V. K. Sharma and X.-Z. Li, Synthesis and photocatalytic activity of ferrites under visible light: a review, *Sep. Purif. Technol.*, **87**, 1 (2012).
8. F. Iqbal, M. I. A. Mutalib, M. S. Shaharun and B. Abdullah, Synthesis of ZnFe₂O₄ using sol-gel method: effect of different calcination parameters, *Procedia Eng.*, **148**, 787 (2016).
9. E. Karamian and S. Sharifnia, On the general mechanism of photocatalytic reduction of CO₂, *J. CO₂ Util.*, **16**, 194 (2016).
10. A. Kezzim, N. Nasrallah, A. Abdi and M. Trari, Visible light induced hydrogen on the novel hetero-system CuFe₂O₄/TiO₂, *Energy Convers. Manag.*, **52**, 2800 (2011).
11. J. Low, B. Cheng, J. Yu and M. Jaroniec, Carbon-based two-dimensional layered materials for photocatalytic CO₂ reduction to solar fuels, *Energy Storage Mater.*, **3**, 24 (2016).
12. Y. Matsumoto, Energy positions of oxide semiconductors and photocatalysis with iron complex oxides, *J. Solid State Chem.*, **126**, 227 (1996).
13. E. Moreira, L. Fraga, M. Mendonça and O. Monteiro, Synthesis, optical, and photocatalytic properties of a new visible-light-active ZnFe₂O₄-TiO₂ nanocomposite material, *J. Nanoparticle Res.*, **14**, 937 (2012).
14. O. Ola and M. M. Maroto-Valer, Review of material design and reactor engineering on TiO₂ photocatalysis for CO₂ reduction, *J. Photochem. Photobiol. C.*, **24**, 16 (2015).
15. G. Rekhila, M. Trari and Y. Bessekhoud, Characterization and application of the hetero-junction ZnFe₂O₄/TiO₂ for Cr (VI) reduction under visible light, *Appl. Water Sci.*, **7**, 1273 (2017).
16. P. J. Huang, K. L. Chang, J.F. Hsieh and S.T. Chen, Catalysis of rice straw hydrolysis by the combination of immobilized cellulase from *Aspergillus niger* on β-cyclodextrin-Fe₃O₄ nanoparticles and ionic liquid, *BioMed Res. Int.*, **2015**, 9 (2015).
17. K. Rajam, S. Rajendran and N. N. Banu, Effect of Caffeine-Zn²⁺ System in Preventing Corrosion of Carbon Steel in Well Water, *J. Chem.*, **2013**, 11 Pages, (2013).
18. W. Kong, A. Wang, J. J. Freeman and P. Sobron, A comprehensive spectroscopic study of synthetic Fe²⁺, Fe³⁺, Mg²⁺ and Al³⁺ copiapite by Raman, XRD, LIBS, MIR and vis-NIR, *J Raman Spectrosc*, **42**, 1120 (2011).
19. M. Tahir and N. S. Amin, Advances in visible light responsive titanium oxide-based photocatalysts for CO₂ conversion to hydrocarbon fuels, *Energy Convers. Manag.*, **76**, 194 (2013).
20. M. R. Uddin, M. R. Khan, M. W. Rahman, A. Yousuf and C. K. Cheng, Photocatalytic reduction of CO₂ into methanol over CuFe₂O₄/TiO₂ under visible light irradiation, *React Kinet Mech Cat.*, **116**, 589 (2015).